

# Non-uniform and anisotropic electric polarizability resulting in pronounced local repulsion minima in high-temperature superconductors

Nassim Derriche and George Sawatzky

*Department of Physics and Astronomy & Stewart Blusson Quantum Matter Institute,  
The University of British Columbia, Vancouver BC, Canada V6T 1Z4*

We demonstrate the dramatic effect of non-uniform, discrete electric polarizability in high- $T_C$  superconductors on the spatial fluctuations of the short to medium range Coulomb interactions through a real-space semiclassical model. Although this is a general property, we concentrate on the cuprates as parent compounds, in which the charge carriers are primarily concentrated on the O sublattice. The anisotropic effective Cu-O bond polarization caused by charge transfer energy modulation and the  $O^{2-}$  atomic polarizability together generate a non-monotonic screened hole-hole Coulomb interaction at short distances that displays a local minimum at the in-plane second nearest neighbor O-O distance solely along the Cu-O bond direction. This is in accordance with the pseudogap phase anisotropy and the short coherence length observed in many high- $T_C$  superconductors.

The study of high-temperature superconductors has been a cornerstone of materials science since the discovery of the first cuprate superconductor in 1986 [1, 2]. The phenomena explaining the properties of this complicated class of compounds remains controversial to date. The underlying physics enabling superconductivity in so-called conventional superconductors is reliably understood from BCS theory to stem from electron-phonon coupling allowing for the electron-electron (or hole-hole) Coulomb repulsion to be overcome, leading to an effective attractive interaction at an inter-electron spacing much larger than the lattice spacing [3]. This attraction can be thought of as stemming from a minimum in the pair energy if the charge carriers are far apart via the exchange of a phonon, as is the case in the Cooper pair formation theory. However, one of the many standing mysteries of the cuprate superconductors is the short measured coherence length, which corresponds to the the average distance between the carriers in a pair [4]. This is hard to justify within the conventional BCS theory since the direct repulsive interaction that has to be overcome would be too large; typical electron-phonon based theories seem not to work. Consequently, an integral focus of the superconducting physics community has been to develop model Hamiltonians which include repulsive interactions and pairing mechanism other than phonons such as spin or charge fluctuations, albeit with limited success [5, 6]. A great deal of very interesting phenomena have been discovered in the exciting path of trying to explain the high- $T_C$  behaviour of cuprates and similar materials like the infinite layer nickelates and iron-based superconductors [7–9].

Through charge susceptibility calculations for a model only containing repulsive interactions, Leggett has shown that an important part of the energy savings caused by pairing in cuprates originates from the enhancement of the small  $q$  (large wavelength) Coulomb interaction screening [10]. This elegant theory predicts an attractive interaction at relatively large distances, a possibility for which he also provides considerable experimental evidence. However, the very short correlation length of a pair in the high- $T_C$  cuprates is an indication that a mechanism acting on a short range is responsible. A candidate that has shown promise in formalizing the theory of high- $T_C$  superconductors is electric polarization in non-uniformly polarizable media [9, 11]. While the proper treatment of polarization is a very well studied topic, it is an area that is often plagued with multiple approximations that mask its full effects [12, 13]. It has been demonstrated that this phenomenon has the potential contribute a strong attractive contribution to short range charged fermionic pair interactions, although the net interaction remained repulsive as shown by publications from Georges and Imada [8, 14]. The example of iron pnictides is based on the very high polarizabilities of the heavy anions arsenic or selenium [9, 15], although Imada and Georges found that charge transfer processes between .

In this paper we show that if we consider the influence of highly-directional bond polarizabilities in addition to atomic polarizabilities, a significant attractive contribution to the internal charge carrier pair interaction arises for the case of holes on oxygen ions in close proximity in the  $CuO_2$  planes. This result is presented in Figure 1, where the inset shows the net interaction between two holes on second nearest neighbor O sites. This effect is highly range and direction-dependent, and results in large local minima and maxima in the inter-oxygen hole-hole interactions. We go beyond the prominent Clausius-Mossotti formulation of polarization in solids, which is a long-standing way of estimating optical dielectric constants via atomic polarizabilities in ionic insulators [16–18]. That approach smooths out the discrete nature of the lattice and defines a dielectric function that describes the screening behavior at large distances ( $q = 0$ ) in a given material; foregoing this approximation can lead to considerable non-monotonic behavior of the two-particle interaction [19, 20]. On the other hand, when it comes to the more covalent materials such as Si, the bond polarizability must also play a very important part in the screening of Coulomb interactions [21, 22]. For these systems whose electronic structure is described very well by density functional methods (DFT), the calculated band structures can also be used to work out the charge susceptibility and the optical dielectric constant using a

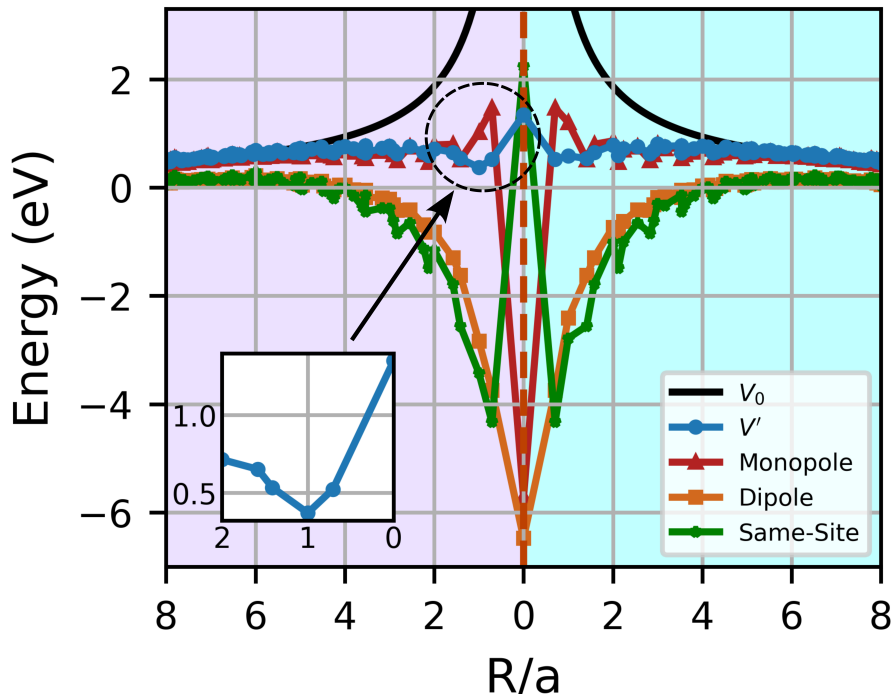


FIG. 1. Effective screened two-hole Coulomb interaction  $V'(\vec{\mathbf{R}}_{h_1}, \vec{\mathbf{R}}_{h_2})$ . This data was computed using equation (8) with realistic base parameters (see text) as a function of distance with  $h_1$  fixed at  $R = 0$  on an O site and  $h_2$  also positioned on an O site along Path 1 (violet, violet region) or Path 2 (right, blue region). A breakdown of the different contributions to  $V'(\vec{\mathbf{R}}_{h_1}, \vec{\mathbf{R}}_{h_2})$  from equation (7) is also shown.

Lindhard function approach. In strongly correlated materials which often are in-between ionic and covalent such as the cuprate superconductors however, these approaches are not expected to work well for calculating short range interactions which, as we will show, are dominated by local field corrections. Furthermore, these local effects are mostly neglected or strongly approximated despite their importance especially for lower-dimensional materials, often by assuming a fully diagonal dielectric matrix [13, 23]. We demonstrate their importance by including not only the atomic polarizability but also the bond polarizability which is responsible for the covalency contribution to the general dielectric function. We focus on the  $\text{CuO}_2$  2D-layer of cuprate superconductors as a principal case study because of it hosting the key physics in those compounds and their historic importance in the field of high- $T_c$  superconductivity, as well as due to the presence of highly-polarizable  $\text{O}^{2-}$  ions and significant covalent bonding between the Cu and O ions [24, 25].

We start with the valuable conclusion of most studies that the mobile charge carriers are primarily housed in O  $2p$  orbitals in the hole-doped cuprates, as in the Zhang-Rice singlet description or the three-spin polaron picture of Emery, because it is widely recognized that the parent compounds are in the charge transfer gap region of the ZSA classification scheme [24, 26, 27]. In this work, we are interested in the screened Coulomb interaction  $V'(\vec{\mathbf{R}}_{h_1}, \vec{\mathbf{R}}_{h_2})$  between two doped holes  $h_1$  and  $h_2$  of charge  $|e|$  located on the ions positioned at  $\vec{\mathbf{R}}_{h_1}$  and  $\vec{\mathbf{R}}_{h_2}$  respectively in an initially undoped  $\text{CuO}_2$  layer cluster with a typical Cu-Cu distance  $a = 3.80 \text{ \AA}$  [28]. This quantity is obtained by subtracting the polarization energy associated with the holes' introduction  $E_{pol}(\vec{\mathbf{R}}_{h_1}, \vec{\mathbf{R}}_{h_2})$  to the bare interaction  $V_0(\vec{\mathbf{R}}_{h_1}, \vec{\mathbf{R}}_{h_2})$ :

$$V'(\vec{\mathbf{R}}_{h_1}, \vec{\mathbf{R}}_{h_2}) = V_0(\vec{\mathbf{R}}_{h_1}, \vec{\mathbf{R}}_{h_2}) - E_{pol}(\vec{\mathbf{R}}_{h_1}, \vec{\mathbf{R}}_{h_2}). \quad (1)$$

We set up an electrostatic model which is illustrated in Figure 2a. The ionic positions  $\vec{\mathbf{R}}_{ij}^\kappa$  are labelled by indices (i,j) which indicate the positions of Cu sites and by index  $\kappa \in \{\text{Cu}, \text{O} \uparrow, \text{O} \rightarrow\}$  that designates an ion in the standard 3-atom basis including a Cu and the O ions above and to its right. All quantities associated with a specific ion follow this indexing scheme below. To compute  $V'(\vec{\mathbf{R}}_{h_1}, \vec{\mathbf{R}}_{h_2})$ , we fix  $h_1$  on a specific ion and vary the position of  $h_2$ .

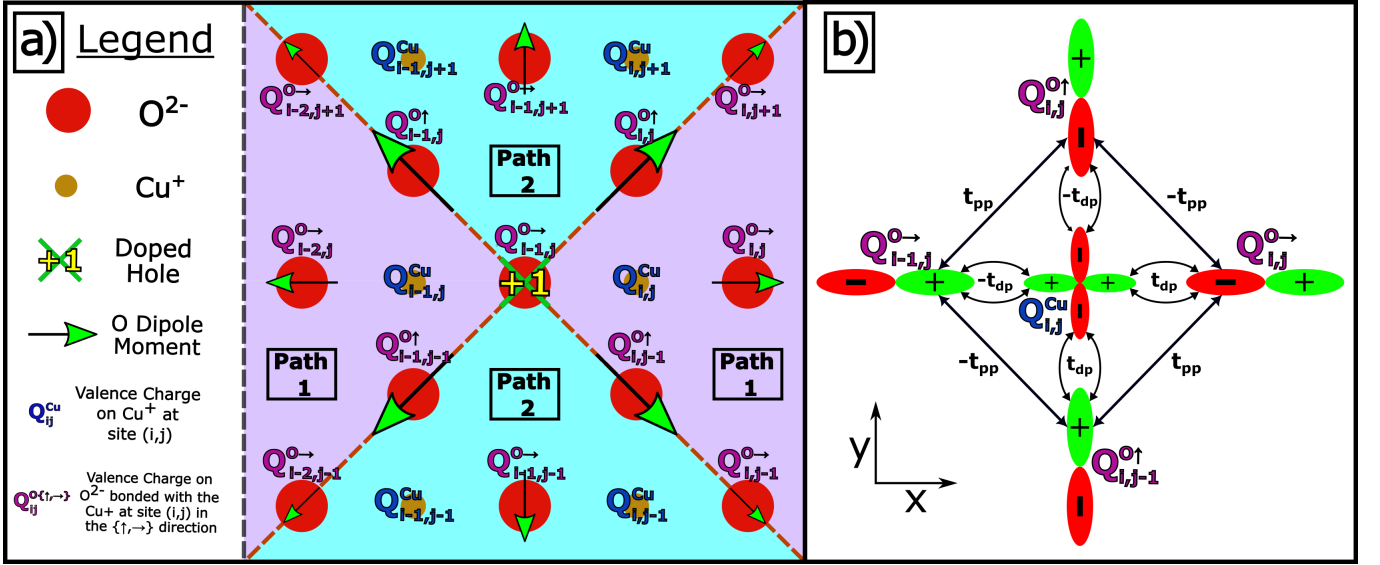


FIG. 2. a) Diagram of the polarization effects induced by a single doped hole on an O site of a  $\text{CuO}_2$  cluster. Calculations with a second hole placed in Paths 1 and 2 were performed to take the angular dependence of the two-particle interaction into account. b) Nearest neighbor hole hopping processes between a single Cu  $3d_{x^2-y^2}$  orbital and its four surrounding O  $2p_x/2p_y$  orbitals. This represents the Hamiltonian in equation (4).

Crucially, when considering doped holes on O sites, there is an angular dependence to the 2-hole interaction caused by the presence of twice as many O ions as Cu ions in the structure, leading to a two-fold rotation-symmetric Coulomb interaction  $V'(\vec{\mathbf{R}}_{h_1}, \vec{\mathbf{R}}_{h_2}) \neq V'(R_{h_2-h_1})$  that it not a pure function of the hole-hole distance  $R_{h_2-h_1} = |\vec{\mathbf{R}}_{h_2} - \vec{\mathbf{R}}_{h_1}|$ . We thus consider the two distinct directions in which  $h_2$  can be placed, namely Path 1 and Path 2 as indicated in Figure 2 a), which respectively does and doesn't feature a Cu ion in between  $h_1$  and  $h_2$  if the latter is placed at the second nearest neighbor O site from  $h_1$  ( $R_{h_2-h_1} = a$ ). The doped holes produce a combined monopole Coulomb electric field  $\vec{\mathbf{E}}_h(\vec{\mathbf{R}}_{ij}^k)$  and a potential  $V_h(\vec{\mathbf{R}}_{ij}^k)$  which electrically polarize ions, inducing atomic electric dipoles  $\vec{\mathbf{p}}_{ij}^k$  which also emit their own collective dipole electric field  $\vec{\mathbf{E}}_p(\vec{\mathbf{R}}_{ij}^k)$  and potential  $V_p(\vec{\mathbf{R}}_{ij}^k)$ . These potentials also modify the on-site energy cost  $\epsilon_{ij}^k$  of adding a hole to a specific ion, leading to a modulation of the charge transfer energy

$$\Delta_{ij}^{\{\uparrow, \rightarrow\}} = \epsilon_{ij}^{O\{\uparrow, \rightarrow\}} - \epsilon_{ij}^{Cu} \quad (2)$$

for each bond. This local covalency-varying effect induces polarization strictly aligned with bond axes which modifies the effective valence hole charge  $Q_{ij}^k$  on each ion, which we take to be point-like. These charges also have their own combined field  $\vec{\mathbf{E}}_Q(\vec{\mathbf{R}}_{ij}^k)$  and potential  $V_Q(\vec{\mathbf{R}}_{ij}^k)$ .

The atomic dipoles have the following linear form:

$$\vec{\mathbf{p}}_{ij}^k = \alpha_O \left( \vec{\mathbf{E}}_h(\vec{\mathbf{R}}_{ij}^k) + \vec{\mathbf{E}}_Q(\vec{\mathbf{R}}_{ij}^k) + \vec{\mathbf{E}}_p(\vec{\mathbf{R}}_{ij}^k) \right), \quad (3)$$

where  $\alpha_O$  is the atomic polarizability of the  $\text{O}^{2-}$  ion. Because of the very small polarizability of the  $\text{Cu}^+$  ions compared to  $\alpha_O$ , its atomic dipoles are inconsequential [29]. On the other hand, determining the changes in the valence hole charge densities on Cu and O ions induced by hole doping is not as simple. As is standard, we consider the hole vacuum state to be populated by  $\text{O}^{2-}$  and  $\text{Cu}^+$  ions such that their electronic configurations ( $2p^6$  and  $3d^{10}$  respectively) only have filled shells [24, 26, 30]. It is known experimentally as well as through *ab initio* calculations that the  $\text{CuO}_2$  planes in undoped cuprates host 1 hole per Cu [28, 31]. While that hole is often taken as being fully on the Cu  $3d$  orbitals, calculations and nuclear magnetic resonance (NMR) measurements have shown a strong covalent character in the wavefunction of that hole; approximately 70% to 80% of its charge density rests on Cu sites, while 20% to 30% is on O ions (corresponding to 10% to 15% per O) [32, 33]. To capture this covalency before and after doping, we set up a local 5-dimensional Hamiltonian  $H_{ij}$  for each "CuO<sub>4</sub>" cluster containing one Cu site and the four O ions surrounding it:

$$\begin{aligned}
H_{ij} &= \Psi_{ij}^\dagger h_{ij} \Psi_{ij}, \\
\Psi_{ij} &= \left( d_{ij} \ p_{ij}^\uparrow \ p_{ij}^\rightarrow \ p_{i,j-1}^\uparrow \ p_{i-1,j}^\rightarrow \right)^T, \\
h_{ij} &= \begin{bmatrix} 0 & -t_{dp} & -t_{dp} & t_{dp} & t_{dp} \\ -t_{dp} & \Delta_{ij}^\uparrow & t_{pp} & 0 & -t_{pp} \\ -t_{dp} & t_{pp} & \Delta_{i-1,j}^\rightarrow & -t_{pp} & 0 \\ t_{dp} & 0 & -t_{pp} & \Delta_{i,j-1}^\uparrow & t_{pp} \\ t_{dp} & -t_{pp} & 0 & t_{pp} & \Delta_{ij}^\rightarrow \end{bmatrix},
\end{aligned} \tag{4}$$

where  $d_{ij}$  and  $p_{ij}^{\{\uparrow, \rightarrow\}}$  are the annihilation operators for a hole on the Cu at (i,j) and on the O at (i,j,O{\uparrow, \rightarrow}) respectively, and  $t_{dp}$  and  $t_{pp}$  are respectively the hopping integrals between neighboring Cu 3d and O 2p orbitals and nearest neighbor O 2p orbitals. A visualization of a cluster along with the phase relationship between orbitals is given in Figure 2 b). The screened charge transfer energies  $\Delta_{ij}^{\{\uparrow, \rightarrow\}}$  depend on the on-site energies  $\epsilon_{ij}$  as shown in equation (2), which can be written as:

$$\epsilon_{ij}^\kappa = |e| \left[ V_h(\vec{\mathbf{R}}_{ij}^\kappa) + V_Q(\vec{\mathbf{R}}_{ij}^\kappa) + V_p(\vec{\mathbf{R}}_{ij}^\kappa) + V_M \right] + U_{ij}^\kappa \tag{5}$$

where  $U_{ij}^\kappa$  is the mean field level same-site contribution to the cost of adding a hole at  $\vec{\mathbf{R}}_{ij}^\kappa$  and  $V_M$  is the Madelung potential in the vacuum state on ion type  $\kappa$  (elaborated in the supplementary note).

Diagonalizing  $h_{ij}$  in equation (4) for all the  $\text{CuO}_4$  clusters included in our model yields their ground states  $\Phi_{ij} = [\Phi_{ij}^{(1)} \ \Phi_{ij}^{(2)} \ \Phi_{ij}^{(3)} \ \Phi_{ij}^{(4)} \ \Phi_{ij}^{(5)}]$ , from which we extract the effective charge density on each ion:

$$\begin{bmatrix} Q_{ij}^{Cu} \\ Q_{ij}^{O\uparrow} \\ Q_{i-1,j}^{O\rightarrow} \\ Q_{i,j-1}^{O\uparrow} \\ Q_{ij}^{O\rightarrow} \end{bmatrix} = |e| \begin{bmatrix} |\Phi_{ij}^{(1)}|^2 \\ |\Phi_{ij}^{(2)}|^2 + |\Phi_{i,j+1}^{(4)}|^2 \\ |\Phi_{ij}^{(3)}|^2 + |\Phi_{i-1,j}^{(5)}|^2 \\ |\Phi_{ij}^{(4)}|^2 + |\Phi_{i,j-1}^{(4)}|^2 \\ |\Phi_{ij}^{(5)}|^2 + |\Phi_{i+1,j}^{(2)}|^2 \end{bmatrix}. \tag{6}$$

To calculate  $E_{pol}(\vec{\mathbf{R}}_{h_1}, \vec{\mathbf{R}}_{h_2})$  from equation (1) for the effective two-hole screened interaction, subtraction of single hole contributions and of the base undoped energy of each cluster is necessary. Let us denote a hole configuration with  $h$  which can indicate the presence of two hole ( $h = h_1 + h_2$ ), a single hole ( $h = h_1$  or  $h = h_2$ ) or no holes ( $h = 0$ ) such that:

$$-E_{pol}^h(\vec{\mathbf{R}}_{h_1}, \vec{\mathbf{R}}_{h_2}) = \sum_{i,j,\kappa} \left[ Q_{ij}^\kappa \left( \frac{V_Q(\vec{\mathbf{R}}_{ij}^\kappa)}{2} + V_h(\vec{\mathbf{R}}_{ij}^\kappa) \right) - \frac{\vec{\mathbf{P}}_{ij}^\kappa}{2} \cdot \left( \vec{\mathbf{E}}_Q(\vec{\mathbf{R}}_{ij}^\kappa) + \vec{\mathbf{E}}_h(\vec{\mathbf{R}}_{ij}^\kappa) \right) + \Omega_{ij}^\kappa \right], \tag{7}$$

$$E_{pol}(\vec{\mathbf{R}}_{h_1}, \vec{\mathbf{R}}_{h_2}) = (E_{pol}^{h_1+h_2} - E_{pol}^0) - (E_{pol}^{h_1} - E_{pol}^0) - (E_{pol}^{h_2} - E_{pol}^0) = E_{pol}^{h_1+h_2} - E_{pol}^{h_1} - E_{pol}^{h_2} + E_{pol}^0, \tag{8}$$

where  $\Omega_{ij}^\kappa$  is the interaction between charges on the same ionic site (see the supplementary note). This includes monopole-monopole, monopole-dipole, dipole-dipole interactions and dipole formation energy.

As realistic parameters in equations (3) and (4), we use literature values obtained from experimental data and tight binding fits to DFT-calculated band structures on cuprates;  $t_{dp}^0 = 1.30$  eV,  $t_{pp}^0 = 0.65$  eV and  $\alpha_O^0 = 2.75 \text{ \AA}^3$  [28, 29, 34]. The charge transfer energy  $\Delta_{ij}^{\{\uparrow, \rightarrow\}}$  in equation (2) however is more complicated to set; it is modulated by polarization effects differently for each Cu-O bond, but a base value  $\Delta^0$  which quantifies the energy cost difference of adding a hole on a  $\text{O}^{2-}$  ion versus a  $\text{Cu}^+$  in the vacuum configuration needs to be chosen. Through calibrating our model such that the right hole covalency is obtained without any doped holes, we set  $\Delta^0 = 6.0$  eV (detailed in the supplementary note). The screened Coulomb potential found with these parameters by solving the non-linear system

of equations formed by equations (3) and (6) is shown in Figure 1. The interaction is significantly non-monotonic at short distances due to the pronounced local field effects caused by the interdependent polarizing influence of the doped holes, the atomic dipoles and the induced changes in ionic valence charges. A pronounced local minimum in the first ( $R_{h_2-h_1} = \frac{a}{\sqrt{2}}$ ) to third ( $R_{h_2-h_1} = \frac{2a}{\sqrt{2}}$ ) nearest neighbor region arises, with the largest dip emerging at the second nearest neighbor distance ( $R_{h_2-h_1} = a = 3.80 \text{ \AA}$ ) if there is a Cu ion directly in between the two hole-occupied O sites. This indicates the existence of a localized suppression of the hole-hole repulsion and is consistent with the short cuprate superconductor coherence length, which is around 10 \AA or smaller [4]. We can reconcile our results with the Allen-Dynes formulation, a semi-analytical way to solve the Eliashberg equations for electron-phonon coupling-mediated superconductors:

$$T_C \propto \exp\left\{\frac{-1.04(1+\lambda)}{\lambda - \mu^*(1+0.62\lambda)}\right\}, \quad (9)$$

where  $\lambda$  is a measure of electron-phonon coupling strength and  $\mu^*$  is the effective electronic Coulomb repulsion [35, 36]. The value of  $\mu^*$  is often set by comparison to experimental or *ab initio* results, with common values ranging between 0.1 and 0.3 depending on the presence of anti-pairing effects competing with superconductivity [37]. However, the fact that it is a singular value makes it fail to capture strong fluctuations in the Coulomb interactions. Equation (9) showcases that a small enough  $\mu^*$  could be the main driver of Cooper pairing even with small  $\lambda$  but also that, even with electron-phonon coupling (or another mechanism entirely) being the principal originator of superconductivity in a material, a highly-screened Coulomb interaction such as the one calculated in this model can significantly enhance  $T_C$ . Local Coulomb energy minima in real space can also still influence coherence lengths based no matter how small their amplitude since they still represent energetically favorable positions, especially at doping densities that make the long range part of  $V'(\vec{\mathbf{R}}_{h_1}, \vec{\mathbf{R}}_{h_2})$  unreachable.

The absence of the pronounced second nearest neighbor local minimum along Path 2 strongly enforces the need to properly take the potential anisotropy of the Coulomb interaction into account in any accurate modelization of short-range phenomena. This anisotropy is displayed in Figure 3. Comparing the left and right columns, the non-linearity of the polarization effects is made obvious; the polarization cloud caused by the simultaneous influence of more than one hole is not equivalent to the superposition of their individual effects, the latter approach resulting in a momentous overestimation of charge and dipole modulation. If we turned off the charge transfer modulation and only calculated polarization through ionic dipoles, the prior statement is true due to the direct addition featured in the right column failing to capture a crucial term  $\propto \vec{\mathbf{E}}_{h_1}(\vec{\mathbf{R}}_{ij}^{\kappa_i}) \cdot \vec{\mathbf{E}}_{h_2}(\vec{\mathbf{R}}_{ij}^{\kappa_j})$  in the polarization energy [38]. Thus, concurrently and interdependently taking the effects of all polarizing sources into account is necessary. Furthermore, through proper subtraction of single particle and vacuum terms, the general orientation of induced dipoles is flipped compared to the right column results as a consequence of the highly nonlinear behavior of the local charge transfer energies. Now focusing on the realistic results on the left column, a) shows that the minimum at  $R_{h_2-h_1} = a$  along Path 1 is caused by the induction of significant same-site negative charge and atomic dipoles whose overall electric force counter the hole-hole repulsion. This is highlighted by comparing Paths 1 and 2 in Figure 1 at  $R_{h_2-h_1} = a$ , especially the dipole and same-site contributions. The monopole part is also anisotropic due to the small negative charge on the middle Cu, albeit to a lesser degree. The magnitude of these effects along Path 2 are quite lower as presented in b). To contrast, the nearest neighbor polarization in c) also exhibits dipoles and charges favourable to hole-hole attraction, explaining the Path 2 local minimum occurring at that distance, but the repulsion suppression is not as strong. These results are consistent with the cuprates being d-wave superconductors and the anisotropy inherent to the experimentally-measured pseudogap phase considered to be intrinsically linked to the superconducting phase of these materials, which exhibits insulating states allowing for Cooper pair formation only along the Cu-O bond direction [39, 40]. Similar pseudogap phases have also been observed in other high- $T_C$  superconductors such pnictides and nickelates [41, 42], but also in conventional superconductors [43, 44] and non-superconducting materials [45], highlighting the broad applicability of this model.

The dependence of  $V'(\vec{\mathbf{R}}_{h_1}, \vec{\mathbf{R}}_{h_2})$  on the model's parameters is also studied in Figure 4. Through a), b) and c) we see that the screening strength is inversely proportional to  $\Delta^0$ ,  $t_{dp}$  and  $\alpha_O$ , which make sense since large values mean that polarization effects will not modulate covalency and atomic dipole magnitudes as strongly relative to the undoped state as illustrated by equations (2) and (5). On the other hand, reducing it leads to the Path 1  $R_{h_2-h_1} = a$  minimum to be attractive, indicating that strong deviations from realistic parameters can lead to unphysical results (such as  $\Delta_{ij}^{\{\uparrow, \rightarrow\}} < 0$  for some Cu-O bonds) and convergence issues, corroborating the model's realism. Thus, similar calculations for other materials necessitate somewhat accurate approximations to Hamiltonian parameters. Furthermore, d) reveals that lowering the nearest neighbor O-O hopping has the peculiar effect of destroying the Path

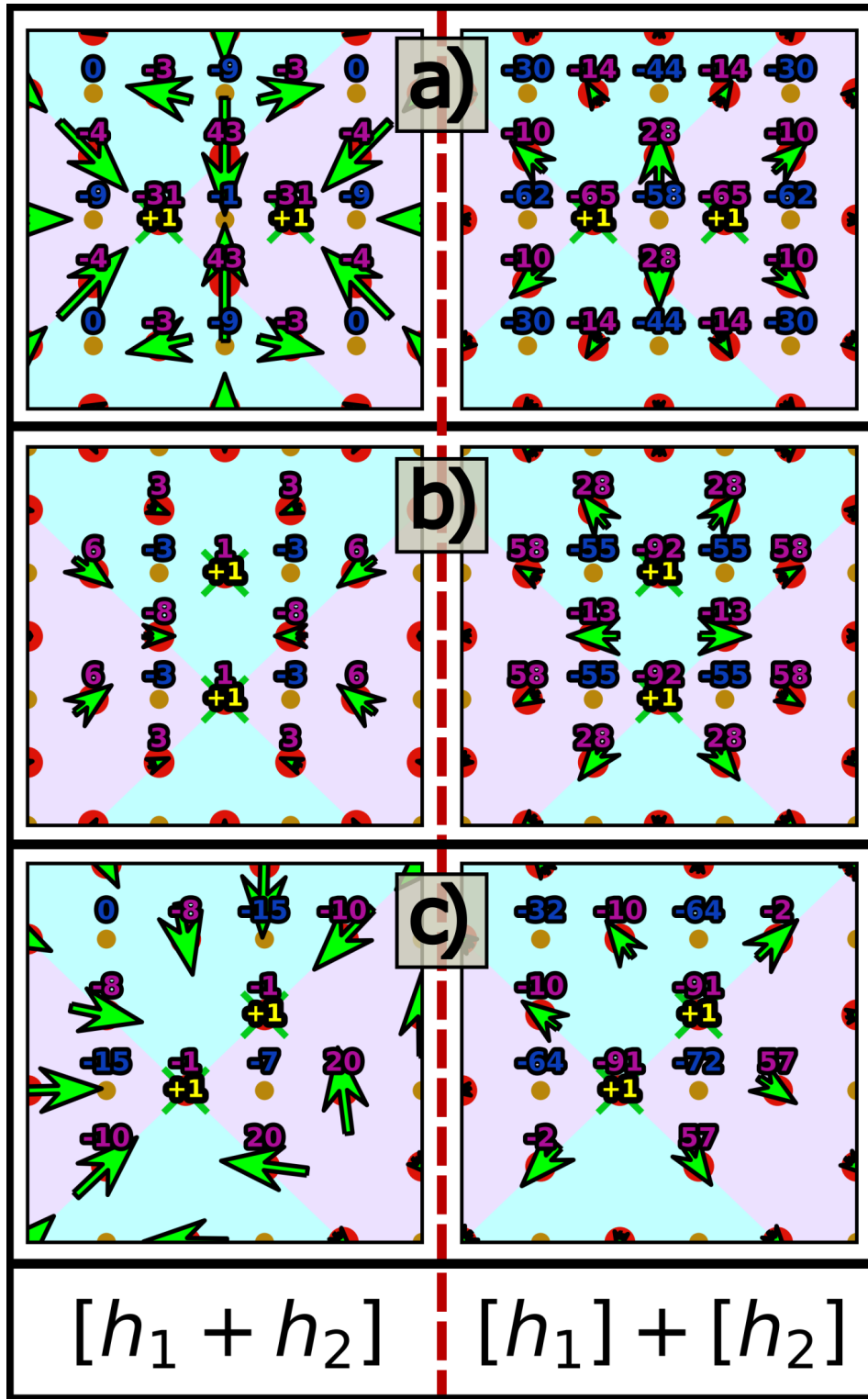


FIG. 3. Induced charge and  $O^{2-}$  dipole modulation induced by the introduction of doped holes. The holes are placed on O sites that are a) second nearest neighbors along Path 1, b) second nearest neighbors along Path 2 and c) nearest neighbors. The results on the left side of the figure result from a calculation with both holes present simultaneously while the one in the right side are from summing the polarization results with  $h_1$  and  $h_2$  placed independently. The charges are in units of  $\frac{|e|}{1000}$ , and the dipole vector lengths on the left side are multiplied by 100 compared to the right side's dipole scale.

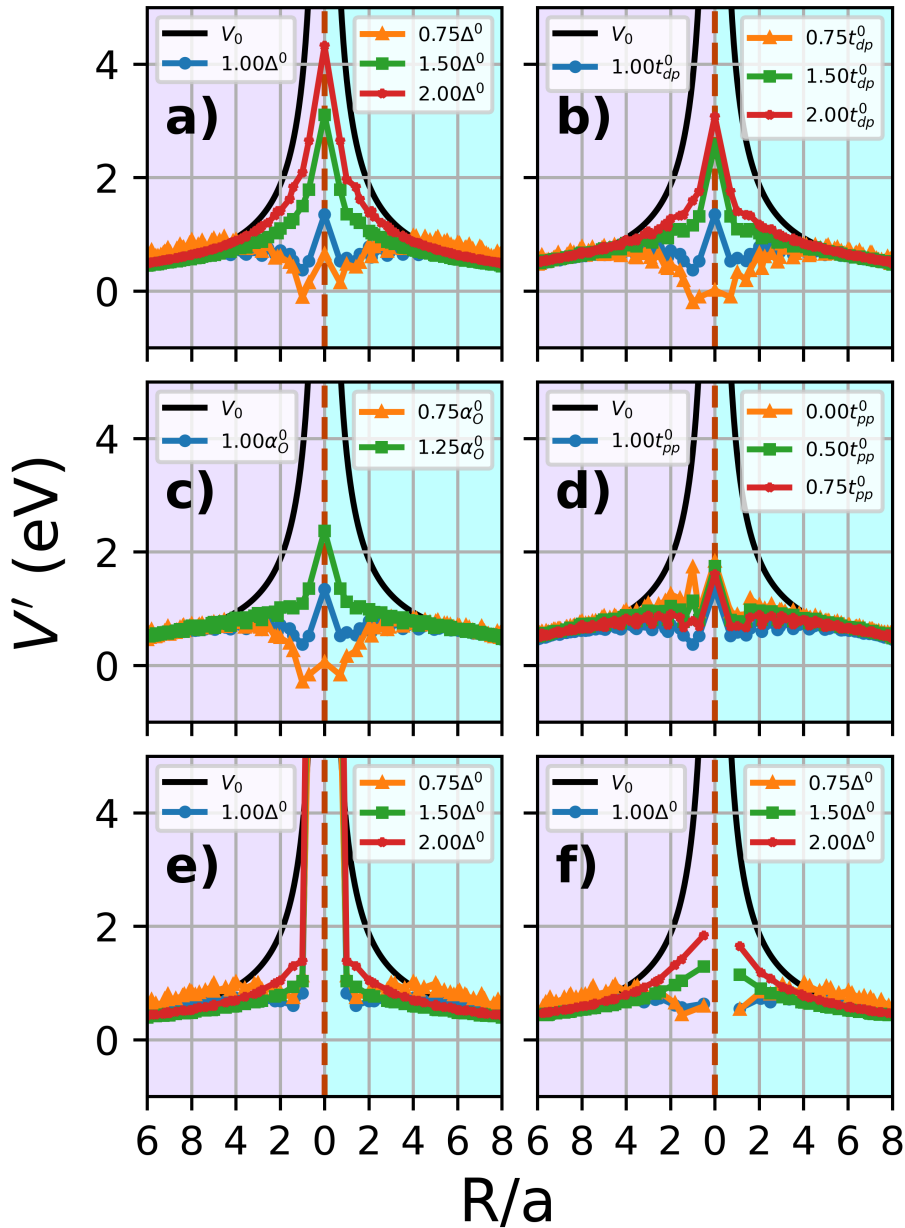


FIG. 4.  $V'(\vec{\mathbf{R}}_{h_1}, \vec{\mathbf{R}}_{h_2})$  calculated for various Hamiltonian parameters and hole ionic combinations. With the two holes on O sites, potentials with different a)  $\Delta^0$ , b)  $t_{dp}$ , c)  $\alpha_O$  and d)  $t_{pp}$  values are shown while keeping all other parameters equal to their base values as listed in the text. The same is presented for varying  $\Delta^0$  for e) both holes on Cu sites, and f)  $h_1$  on an O site and  $h_2$  on a Cu site.

1 local minimum and even turn it into a maximum. Physically, the O-O hopping channel dying out means that more Cu-O transfer occurs, causing a large building of positive charge on the middle Cu which repels the holes and elevates the monopole and same-site parts of  $V'(\vec{\mathbf{R}}_{h_1}, \vec{\mathbf{R}}_{h_2})$ . Finally, e) and f) show that a small local minimum also occurs when at least one hole is placed on a Cu site instead of O, which is known to be an energetically unlikely to occur for cuprates in the superconducting doping concentration range. It is interesting to note that there is no anisotropy in the Cu-Cu interaction, but there is an appreciable difference between Paths 1 and 2 present in the O-Cu interaction. Figure 4 shows the absence of long range screening characteristic to 1D and 2D materials since a long-range dielectric constant cannot be defined for dimensions lower than three, but on the other hand low-dimensional systems usually exhibit stronger local field effects [46, 47].

Another central takeaway of this work is that for calculations such as these where or other short-range phenomena are important to properly capture, a real-space approach can offer significant computational advantages. Through a standard *ab initio* reciprocal space calculation, a large amount of reciprocal lattice vectors (G-vectors) needs to be considered to probe both large and small length scale effects simultaneously, leading to the necessary diagonalization of momentously large matrices. To model phenomena down to a length scale  $d$  in a 2D square system with lattice constant  $a$ , all G-vectors  $\vec{\mathbf{G}}_{n_x, n_y} = \frac{2\pi}{a}[n_x, n_y]$  (where  $n_x$  and  $n_y$  are integers) such that  $|\vec{\mathbf{G}}_{n_x, n_y} + \vec{\mathbf{G}}_{n'_x, n'_y}|$  falls within a circle of radius  $\frac{2\pi}{d}$  need to be considered:

$$\sqrt{(n_x + n'_x)^2 + (n_y + n'_y)^2} \leq \frac{a}{d}. \quad (10)$$

To capture the prized second nearest-neighbor ( $d = 3.80 \text{ \AA}$ ) repulsion minimum in a reciprocal space calculation, a large supercell needs to be defined depending on the desired hole doping; at the optimal 0.15 holes per Cu doping for superconductivity, we need  $a = 52.20 \text{ \AA}$  to have 2 holes per cell, [25]. Using equation (10) and only considering vectors that respect  $\vec{\mathbf{G}}_{n_x, n_y} \leq \frac{4\pi}{d}$  leads to 3249 mandatory G-vectors. Similar computations in 3D materials are significantly more expensive in reciprocal space. If one is exclusively interested in what happens in the neighborhood of  $R_{h_2-h_1} = d$ , including non-diagonal elements only for G-vectors in a small spherical shell around radius  $|\vec{\mathbf{G}}_{n_x, n_y}| \approx \frac{2\pi}{d}$  while keeping the other parts of the matrix diagonal leads to size reductions. Regardless, the number of non-diagonal contributions is substantially greater for small  $d$  since there are more combinations  $|\vec{\mathbf{G}}_{n_x, n_y} + \vec{\mathbf{G}}_{n'_x, n'_y}| \approx \frac{2\pi}{d}$ , reducing the potential savings and improving the appeal of a real space approach.

Our model and results pave the way for proper, real-space treatment of the screened fermionic Coulomb interaction in other materials, especially unconventional superconductors that feature highly polarizable ions and non-trivial covalency. Systems with measured pseudogap-like phases like the iron pnictides or nickelates are good candidates to probe the important impact of local field effects. A further extension to this study is to analyze the dependence of  $T_C$  on hole doping concentration, similarly to the doping-dependent paraelectric phase decline in  $\text{SrTiO}_3$  which has been recently studied [48].

This research was undertaken thanks in part to funding from the Max Planck-UBC-UTokyo Center for Quantum Materials and the Canada First Research Excellence Fund, Quantum Materials and Future Technologies Program, as well as by the Natural Sciences and Engineering Research Council (NSERC) for Canada.

- 
- [1] J. G. Bednorz and K. A. Muller, *Zeitschrift fur Physik B Condensed Matter* **64**, 189 (1986), ISSN 0722-3277, iISBN: 9789814293365, URL <http://link.springer.com/10.1007/BF01303701>.
  - [2] J. L. MacManus-Driscoll and S. C. Wimbush, *Nature Reviews Materials* **6**, 587 (2021), ISSN 2058-8437, URL <https://www.nature.com/articles/s41578-021-00290-3>.
  - [3] J. Bardeen, L. N. Cooper, and J. R. Schrieffer, *Physical Review* **108**, 1175 (1957), ISSN 0031-899X, URL <https://link.aps.org/doi/10.1103/PhysRev.108.1175>.
  - [4] J. Hwang, *Scientific Reports* **11**, 11668 (2021), ISSN 2045-2322, URL <https://www.nature.com/articles/s41598-021-91163-w>.
  - [5] S. Caprara, C. Di Castro, G. Seibold, and M. Grilli, *Physical Review B* **95**, 15 (2017), ISSN 24699969, arXiv: 1604.07852, URL <https://journals.aps.org/prb/abstract/10.1103/PhysRevB.95.224511>.
  - [6] J. H. Koo, J.-H. Kim, J.-M. Jeong, G. Cho, and J.-J. Kim, *Modern Physics Letters B* **23**, 1533 (2009), ISSN 0217-9849, URL <https://www.worldscientific.com/doi/abs/10.1142/S0217984909019697>.
  - [7] D. Li, K. Lee, B. Y. Wang, M. Osada, S. Crossley, H. R. Lee, Y. Cui, Y. Hikita, and H. Y. Hwang, *Nature* **572**, 624 (2019), ISSN 0028-0836, URL <https://www.nature.com/articles/s41586-019-1496-5>.
  - [8] M. Aichhorn, S. Biermann, T. Miyake, A. Georges, and M. Imada, *Physical Review B* **82**, 064504 (2010), ISSN 1098-0121, URL <https://link.aps.org/doi/10.1103/PhysRevB.82.064504>.
  - [9] G. A. Sawatzky, I. S. Elfimov, J. Van Den Brink, and J. Zaanen, *Epl* **86** (2009), ISSN 02955075, arXiv: 0808.1390, URL <https://iopscience.iop.org/article/10.1209/0295-5075/86/17006>.
  - [10] A. J. Leggett, *Proceedings of the National Academy of Sciences* **96**, 8365 (1999), ISSN 0027-8424, URL <https://www.pnas.org/doi/10.1073/pnas.96.15.8365>.
  - [11] C. J. Humphreys, *Acta Crystallographica Section A: Foundations of Crystallography* **55**, 228 (1999), ISSN 01087673, publisher: International Union of Crystallography, URL <https://pubmed.ncbi.nlm.nih.gov/10927254/>.
  - [12] I. I. Mazin and R. E. Cohen, *Ferroelectrics* (1997), ISSN 00150193, URL <https://www.tandfonline.com/doi/pdf/10.1080/00150199708016098>.
  - [13] E. G. Maksimov and I. I. Mazin, *Solid State Communications* **27**, 527 (1978), ISSN 00381098, URL <https://www.sciencedirect.com/science/article/abs/pii/0038109878903873>.

- [14] T. Miyake, K. Nakamura, R. Arita, and M. Imada, *Journal of the Physical Society of Japan* **79**, 044705 (2010), ISSN 0031-9015, URL <https://journals.jps.jp/doi/10.1143/JPSJ.79.044705>.
- [15] Y. Yacoby, D. Ceresoli, L. Giordano, and Y. Shao-Horn, arXiv (2021), ISSN 23318422, URL <https://arxiv.org/abs/2105.05124>.
- [16] R. Clausius, *Die Mechanische Behandlung der Electricität* (Vieweg+Teubner Verlag, Wiesbaden, 1879), ISBN 978-3-663-19891-8, URL <http://link.springer.com/10.1007/978-3-663-20232-5>.
- [17] O. F. Mossotti, in *Memorie di Matematica e di Fisica della Società Italiana delle Scienze Residente in Modena* (Società Italiana Delle Scienze, 1850), vol. 24, pp. 49–74, URL <https://www.biodiversitylibrary.org/item/34306#page/1/mode/1up>.
- [18] D. A. Robinson, *Soil Science Society of America Journal* **68**, 1780 (2004), ISSN 0361-5995, URL <https://access.onlinelibrary.wiley.com/doi/10.2136/sssaj2004.1780>.
- [19] G. Brocks, J. van den Brink, and A. F. Morpurgo, *Physical Review Letters* **93**, 146405 (2004), ISSN 0031-9007, URL <https://journals.aps.org/prl/abstract/10.1103/PhysRevLett.93.146405>.
- [20] T. R. Durrant, S. T. Murphy, M. B. Watkins, and A. L. Shluger, *The Journal of Chemical Physics* **149** (2018), ISSN 0021-9606, URL <https://pubs.aip.org/aip/jcp/article/149/2/024103/196619>.
- [21] G. Nagarajan, *Zeitschrift für Naturforschung A* **21**, 238 (1966), ISSN 1865-7109, URL <https://www.degruyter.com/document/doi/10.1515/zna-1966-0308/html>.
- [22] E. Bustarret, C. Marcenat, P. Achatz, J. Kačmarčík, F. Lévy, A. Huxley, L. Ortéga, E. Bourgeois, X. Blase, D. Débarre, et al., *Nature* **444**, 465 (2006), ISSN 0028-0836, URL <https://www.nature.com/articles/nature05340>.
- [23] Y. Litman, F. P. Bonafé, A. Akkoush, H. Appel, and M. Rossi, *The Journal of Physical Chemistry Letters* **14**, 6850 (2023), ISSN 1948-7185, URL <https://pubs.acs.org/doi/10.1021/acs.jpcllett.3c01216>.
- [24] F. C. Zhang and T. M. Rice, *Physical Review B* **37**, 3759 (1988), ISSN 01631829, URL <https://journals.aps.org/prb/abstract/10.1103/PhysRevB.37.3759>.
- [25] C.-T. Chen, Ph.D. thesis, California Institute of Technology (2006), URL <https://thesis.library.caltech.edu/1943/>.
- [26] V. J. Emery, *Physical Review Letters* **58**, 2794 (1987), ISSN 0031-9007, URL <https://link.aps.org/doi/10.1103/PhysRevLett.58.2794>.
- [27] J. Zaanen, G. A. Sawatzky, and J. W. Allen, *Physical Review Letters* **55**, 418 (1985), ISSN 0031-9007, URL <https://journals.aps.org/prl/abstract/10.1103/PhysRevLett.55.418>.
- [28] A. K. McMahan, J. F. Annett, and R. M. Martin, *Physical Review B* **42**, 6268 (1990), ISSN 0163-1829, URL <https://link.aps.org/doi/10.1103/PhysRevB.42.6268>.
- [29] J. R. Tessman, A. H. Kahn, and W. Shockley, *Physical Review* **92**, 890 (1953), ISSN 0031-899X, URL <https://journals.aps.org/pr/abstract/10.1103/PhysRev.92.890>.
- [30] M. S. Golden, C. Dürr, A. Koitzsch, S. Legner, Z. Hu, S. Borisenko, M. Knupfer, and J. Fink, *Journal of Electron Spectroscopy and Related Phenomena* **117-118**, 203 (2001), ISSN 0368-2048, URL <https://www.sciencedirect.com/science/article/pii/S0368204801002663>.
- [31] G. Shirane, Y. Endoh, R. J. Birgeneau, M. A. Kastner, Y. Hidaka, M. Oda, M. Suzuki, and T. Murakami, *Physical Review Letters* **59**, 1613 (1987), ISSN 0031-9007, URL <https://pubmed.ncbi.nlm.nih.gov/10035281/>.
- [32] A. Macridin, M. Jarrell, T. Maier, and G. A. Sawatzky, *Physical Review B - Condensed Matter and Materials Physics* **71** (2005), ISSN 10980121, arXiv: [cond-mat/0411092](https://arxiv.org/abs/cond-mat/0411092), URL <https://journals.aps.org/prb/abstract/10.1103/PhysRevB.71.134527>.
- [33] J. Haase, O. P. Sushkov, P. Horsch, and G. V. M. Williams, *Physical Review B* **69**, 094504 (2004), ISSN 1098-0121, URL <https://journals.aps.org/prb/abstract/10.1103/PhysRevB.69.094504>.
- [34] M. Ogata and H. Fukuyama, *Reports on Progress in Physics* **71**, 036501 (2008), ISSN 0034-4885, URL <https://iopscience.iop.org/article/10.1088/0034-4885/71/3/036501>.
- [35] G. Eliashberg, *Sov. Phys. - JETP* **11:3** (1960), URL <https://www.osti.gov/biblio/7354388>.
- [36] P. B. Allen and R. C. Dynes, *Physical Review B* **12**, 905 (1975), ISSN 0556-2805, URL <https://journals.aps.org/prb/abstract/10.1103/PhysRevB.12.905>.
- [37] E. A. Drzazga, I. A. Domagalska, M. W. Jarosik, R. Szczesniak, and J. K. Kalaga, *Journal of Superconductivity and Novel Magnetism* **31**, 1029 (2018), ISSN 1557-1939, URL <https://link.springer.com/article/10.1007/s10948-017-4295-y>.
- [38] M. Berciu, I. Elfimov, and G. A. Sawatzky, *Physical Review B* **79**, 214507 (2009), ISSN 1098-0121, URL <https://journals.aps.org/prb/abstract/10.1103/PhysRevB.79.214507>.
- [39] V. Aji, A. Shekhter, and C. M. Varma, *Physical Review B* **81**, 064515 (2010), ISSN 1098-0121, URL <https://link.aps.org/doi/10.1103/PhysRevB.81.064515>.
- [40] H. Alloul, T. Ohno, and P. Mendels, *Physical Review Letters* **63**, 1700 (1989), ISSN 0031-9007, URL <https://journals.aps.org/prl/abstract/10.1103/PhysRevLett.63.1700>.
- [41] T. Shimojima, T. Sonobe, W. Malaeb, K. Shinada, A. Chainani, S. Shin, T. Yoshida, S. Ideta, A. Fujimori, H. Kumigashira, et al., *Physical Review B* **89**, 045101 (2014), ISSN 1098-0121, URL <https://journals.aps.org/prb/abstract/10.1103/PhysRevB.89.045101>.
- [42] D. Zhao, Y. Zhou, Y. Fu, L. Wang, X. Zhou, H. Cheng, J. Li, D. Song, S. Li, B. Kang, et al., *Physical Review Letters* **126**, 197001 (2021), ISSN 0031-9007, URL <https://journals.aps.org/prl/abstract/10.1103/PhysRevLett.126.197001>.
- [43] U. S. Pracht, N. Bachar, L. Benfatto, G. Deutscher, E. Farber, M. Dressel, and M. Scheffler, *Physical Review B* **93**, 100503 (2016), ISSN 2469-9950, URL <https://journals.aps.org/prb/abstract/10.1103/PhysRevB.93.100503>.
- [44] M. Mondal, A. Kamlapure, M. Chand, G. Saraswat, S. Kumar, J. Jesudasan, L. Benfatto, V. Tripathi, and P. Raychaudhuri, *Physical Review Letters* **106**, 047001 (2011), ISSN 0031-9007, URL <https://journals.aps.org/prl/abstract/10.1103/>

[PhysRevLett.106.047001](#).

- [45] N. Mannella, W. L. Yang, X. J. Zhou, H. Zheng, J. F. Mitchell, J. Zaanen, T. P. Devereaux, N. Nagaosa, Z. Hussain, and Z.-X. Shen, *Nature* **438**, 474 (2005), ISSN 0028-0836, URL <https://www.nature.com/articles/nature04273#citeas>.
- [46] L. V. Keldysh, *Pis'ma Zh. Eksp. Teor. Fiz.* **29**, 716 (1979), URL [https://www.worldscientific.com/doi/10.1142/9789811279461\\_0024](https://www.worldscientific.com/doi/10.1142/9789811279461_0024).
- [47] E. A. Andryushin, L. V. Keldysh, V. A. Sanina, and A. P. Silin, *Zh. Eksp. Teor. Fiz.* **79**, 1509 (1980), URL [http://www.jetp.ras.ru/cgi-bin/dn/e\\_052\\_04\\_0761.pdf](http://www.jetp.ras.ru/cgi-bin/dn/e_052_04_0761.pdf).
- [48] B. Fauqué, S. Jiang, T. Fennell, B. Roessli, A. Ivanov, C. Roux-Byl, B. Baptiste, P. Bourges, K. Behnia, and Y. Tomioka, *The polarisation fluctuation length scale shaping the superconducting dome of SrTiO<sub>3</sub>* (2024), arXiv:2404.04154 [cond-mat], URL <http://arxiv.org/abs/2404.04154>.

**Supplementary Note 1: Elaboration on the system of nonlinear equations for polarization variables**

For the electric fields and potentials associated with the doped holes, ionic valence charges and atomic dipoles featured in the main text, we have used the following explicit form in CGS units in our numerical computations:

$$\begin{aligned}
V_0(\vec{\mathbf{R}}_{h_1}, \vec{\mathbf{R}}_{h_2}) &= \frac{|e|}{|\vec{\mathbf{R}}_{h_2} - \vec{\mathbf{R}}_{h_1}|} \delta_{\vec{\mathbf{R}}_{h_2}, \vec{\mathbf{R}}_{h_1}}, \\
V_h(\vec{\mathbf{R}}_{ij}^\kappa) &= |e| \sum_{l=1}^2 \frac{1}{|\vec{\mathbf{R}}_{ij}^\kappa - \vec{\mathbf{R}}_{h_l}|} \delta_{\vec{\mathbf{R}}_{ij}^\kappa, \vec{\mathbf{R}}_{h_l}}, \\
\vec{\mathbf{E}}_h(\vec{\mathbf{R}}_{ij}^\kappa) &= |e| \sum_{l=1}^2 \frac{\vec{\mathbf{R}}_{ij}^\kappa - \vec{\mathbf{R}}_{h_l}}{|\vec{\mathbf{R}}_{ij}^\kappa - \vec{\mathbf{R}}_{h_l}|^3} \delta_{\vec{\mathbf{R}}_{ij}^\kappa, \vec{\mathbf{R}}_{h_l}}, \\
V_Q(\vec{\mathbf{R}}_{ij}^\kappa) &= \sum_{(i',j',\kappa') \neq (i,j,\kappa)} Q_{i'j'}^{\kappa'} \frac{1}{|\vec{\mathbf{R}}_{ij}^\kappa - \vec{\mathbf{R}}_{i'j'}^{\kappa'}|}, \\
\vec{\mathbf{E}}_Q(\vec{\mathbf{R}}_{ij}^\kappa) &= \sum_{(i',j',\kappa') \neq (i,j,\kappa)} Q_{i'j'}^{\kappa'} \frac{\vec{\mathbf{R}}_{ij}^\kappa - \vec{\mathbf{R}}_{i'j'}^{\kappa'}}{|\vec{\mathbf{R}}_{ij}^\kappa - \vec{\mathbf{R}}_{i'j'}^{\kappa'}|^3}, \\
V_p(\vec{\mathbf{R}}_{ij}^\kappa) &= \sum_{(i',j',\kappa') \neq (i,j,\kappa)} \frac{\vec{\mathbf{p}}_{i'j'}^{\kappa'} \cdot (\vec{\mathbf{R}}_{ij}^\kappa - \vec{\mathbf{R}}_{i'j'}^{\kappa'})}{|\vec{\mathbf{R}}_{ij}^\kappa - \vec{\mathbf{R}}_{i'j'}^{\kappa'}|^3}, \\
\vec{\mathbf{E}}_p(\vec{\mathbf{R}}_{ij}^\kappa) &= \sum_{(i',j',\kappa') \neq (i,j,\kappa)} \frac{3[\vec{\mathbf{p}}_{i'j'}^{\kappa'} \cdot (\vec{\mathbf{R}}_{ij}^\kappa - \vec{\mathbf{R}}_{i'j'}^{\kappa'})](\vec{\mathbf{R}}_{ij}^\kappa - \vec{\mathbf{R}}_{i'j'}^{\kappa'})}{|\vec{\mathbf{R}}_{ij}^\kappa - \vec{\mathbf{R}}_{i'j'}^{\kappa'}|^5} - \frac{\vec{\mathbf{p}}_{i'j'}^{\kappa'}}{|\vec{\mathbf{R}}_{ij}^\kappa - \vec{\mathbf{R}}_{i'j'}^{\kappa'}|^3}.
\end{aligned} \tag{S.11}$$

The same-site energy cost that enters in equation (2) in the main text is defined as such:

$$U_{ij}^\kappa = \frac{Q_{ij}^\kappa}{|e|} [I^\kappa(n_{ij}^h + \gamma^\kappa + 1) - I^\kappa(n_{ij}^h + \gamma^\kappa)] + I^\kappa(n_{ij}^h + \gamma^\kappa), \tag{S.12}$$

$$I^\kappa(n) = \begin{cases} E_I^\kappa(n+1) & , n \geq 0 \\ -E_A^\kappa(|n|) & , n < 0 \end{cases}, \tag{S.13}$$

where  $E_I^\kappa(n)$  and  $E_A^\kappa(n)$  are respectively the standard  $n^{\text{th}}$  atomic ionization energy and electron affinity of the element labeled by  $\kappa$ ,  $\gamma^\kappa = \delta_{\kappa, Cu} - 2\delta_{\kappa, O\{\uparrow, \rightarrow\}}$  is the oxidation number of the ion considered and  $n_{ij}^h = \sum_{n=1}^2 \delta_{\vec{\mathbf{R}}_{ij}^\kappa, \vec{\mathbf{R}}_{h_n}}$  is the number of doped holes at site  $\vec{\mathbf{R}}_{ij}^\kappa$ . Physically, this means that the cost of adding a hole to an ion with overall charge  $\gamma^\kappa + Q_{ij}^\kappa$  will be an appropriate fraction of the relevant ionization potential or electron affinity, added to one minus that fraction of the next ionization potential or electron affinity [1]. For example, the cost of adding a hole to  $O^{(2-)+0.25} = O^{1.75-}$  is the sum of the costs of the steps  $O^{1.75-} \rightarrow O^{1-}$  and  $O^{1-} \rightarrow O^{0.75-}$ , i.e.  $-0.75E_A^O(2) - 0.25E_A^O(1)$ . The literature energy values that end up being used in this model's numerical calculations are  $E_I^O(1) = 13.62$  eV [2],  $E_I^O(2) = 35.12$  eV [2],  $E_A^O(1) = -1.46$  eV [3],  $E_A^O(2) = 7.71$  eV [4],  $E_I^{Cu}(1) = 7.72$  eV [5],  $E_I^{Cu}(2) = 20.29$  eV [6],  $E_I^{Cu}(3) = 36.84$  eV [7]. The Madelung potential  $V_M^\kappa$  in equation (2) is the potential on the ion type labelled by  $\kappa$  due to all other charges in the cuprate lattice in the vacuum state, in which the  $\text{CuO}_2$  planes (including the apical oxygen) are entirely populated by  $O^{2-}$  and  $\text{Cu}^+$  ions. It also appears in the base, undoped charge transfer energy:

$$\Delta^0 = -E_I^O(2) - E_A^{Cu}(2) + |e|(V_M^O - V_M^{Cu}). \tag{S.14}$$

Next, A disambiguation of what "charge transfer energy" means in this work in contrast to other models is necessary. A common value chosen to reproduce DFT band structures is 3.6 eV, but this would not be applicable to our model because in theory this number should already takes screening effects into account in order to obtain the "real" energy

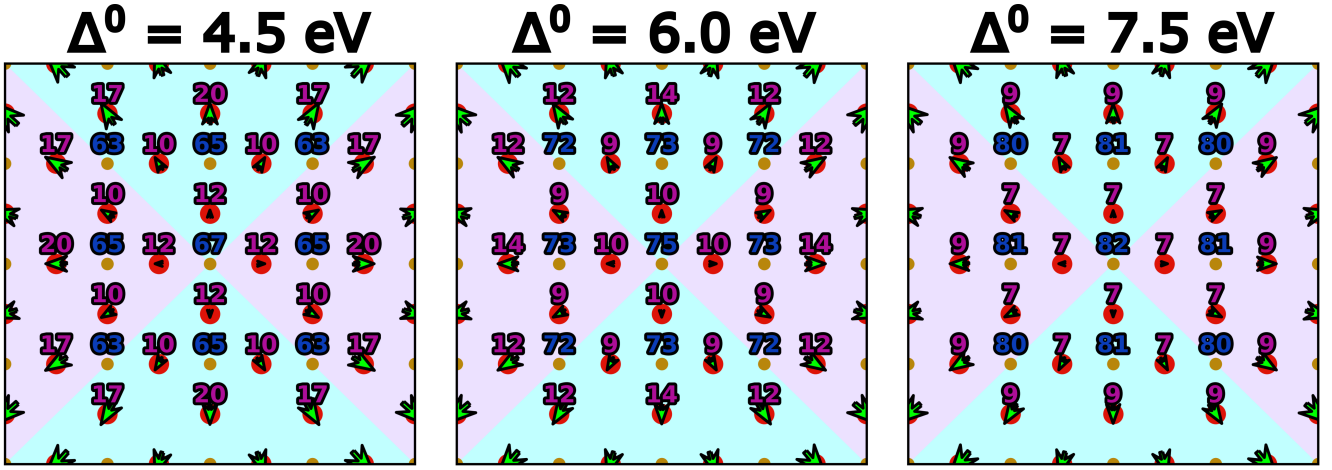


FIG. S.5. Ionic valence charges in an undoped  $\text{CuO}_2$  plane for different values of  $\Delta^0$ . This figure follows the same legend as in Figure 2 in the main text. Small  $\text{O}^{2-}$  atomic dipoles are present as a consequence of the finite nature of the clusters.

dispersion, as well as due to being used in Hamiltonians that do not explicitly consider all Coulomb interactions [8–10]. Consequently, such models attribute the same energy cost to adding a hole on any  $\text{O}^{2-}$  site (except same-site and sometimes nearest-neighbor interactions) despite the effective potential at distinct ionic sites potentially being different due to other added particles and their polarizing influence. This approximation is intrinsically related to the Clausius-Mossotti local field effect-smoothing approach that our model is going beyond. Therefore, instead of using a literature value, we calibrate the Madelung potentials in Equation S.14 (which are hard to calculate from first principles in the vacuum state since they also depend on contributions outside the  $\text{CuO}_2$  plane) such that our model leads to a proper and realistic Cu-O covalency for each hole per Cu added to the vacuum in the undoped  $\text{CuO}_2$  plane. We set  $V_M^O = -V_M^{Cu}$ , a reasonable approximation based on literature calculations for various cuprates [11]. Aiming for a Cu hole density of 75% as a compromise between the different calculation and NMR results cited above, we reach as a baseline value  $\Delta^0 = 6.0$  eV as shown in Figure S.5, specifically looking at the central Cu since edge effects are eliminated and it is influenced by other charges isotropically. This leads to  $|e|V_M^O = 17$  eV and  $|e|V_M^{Cu} = -17$  eV. Furthermore, the screened charge transfer energy  $\Delta_{ij}^\kappa$  we obtain for the undoped system is 1.62 eV, which is in the 1.5-2.0 eV range in which experimentally measured cuprate charge transfer energies fall [11–13].

On the other hand, the same-site term that enters in the polarization energy as featured in equation (7) is slightly different because there can be two doped holes on the same site:

$$\Omega_{ij}^\kappa = \sum_{n=0}^{n_{ij}^h} I^\kappa(n + \gamma) \left[ \left( \frac{Q_{ij}^\kappa}{|e|} - 1 \right) \delta_{n, n_{ij}^h} + 1 \right]. \quad (\text{S.15})$$

With all of these variables defined, the roots of a system of equations are determined numerically using the fsolve function as part of the Python scientific package SciPy [14]. These are then inputted into equation (10) of the main text to calculate the polarization energy of a given hole configuration.

- 
- [1] A. Macridin, M. Jarrell, T. Maier, and G. A. Sawatzky, *Physical Review B - Condensed Matter and Materials Physics* **71** (2005), ISSN 10980121, arXiv: [cond-mat/0411092](https://arxiv.org/abs/cond-mat/0411092), URL <https://journals.aps.org/prb/abstract/10.1103/PhysRevB.71.134527>.
  - [2] R. L. Kelly and L. J. Palumbo, Tech. Rep. NRL-7599, Naval Research Lab., Washington, D.C. (USA) (1973), URL <https://www.osti.gov/biblio/4332843>.
  - [3] M. K. Kristiansson, K. Chartkunchand, G. Eklund, O. M. Hole, E. K. Anderson, N. de Ruelle, M. Kamińska, N. Punnakayathil, J. E. Navarro-Navarrete, S. Sigurdsson, et al., *Nature Communications* **13**, 5906 (2022), ISSN 2041-1723, URL <https://www.nature.com/articles/s41467-022-33438-y>.
  - [4] R. L. K. James E. Huheey, Ellen A. Keiter, *Inorganic Chemistry Principles of Structure and Rela-*

- tivity* (HarperCollins, New York, 1993), URL <https://www.semanticscholar.org/paper/Inorganic-chemistry%3B-principles-of-structure-and-Huheey/c0f189ba30e082b6ddfa98dc03dbd1d17d39f1b6>.
- [5] J. Sugar and A. Musgrove, Journal of Physical and Chemical Reference Data **19**, 527 (1990), ISSN 0047-2689, 1529-7845, URL <https://pubs.aip.org/jpr/article/19/3/527/457273/Energy-Levels-of-Copper-Cu-I-through-Cu-XXIXENERGY>.
- [6] A. Kramida, G. Nave, and J. Reader, Atoms **5**, 9 (2017), ISSN 2218-2004, URL <http://www.mdpi.com/2218-2004/5/1/9>.
- [7] J. Sugar and A. Musgrove, Journal of Physical and Chemical Reference Data **19**, 527 (1990), ISSN 0047-2689, URL <https://pubs.aip.org/jpr/article/19/3/527/457273/Energy-Levels-of-Copper-Cu-I-through-Cu-XXIXENERGY>.
- [8] M. Ogata and H. Fukuyama, Reports on Progress in Physics **71**, 036501 (2008), ISSN 0034-4885, URL <https://iopscience.iop.org/article/10.1088/0034-4885/71/3/036501>.
- [9] A. K. McMahan, J. F. Annett, and R. M. Martin, Physical Review B **42**, 6268 (1990), ISSN 0163-1829, URL <https://link.aps.org/doi/10.1103/PhysRevB.42.6268>.
- [10] F. C. Zhang and T. M. Rice, Physical Review B **37**, 3759 (1988), ISSN 01631829, URL <https://journals.aps.org/prb/abstract/10.1103/PhysRevB.37.3759>.
- [11] A. Tsukada, H. Shibata, M. Noda, H. Yamamoto, and M. Naito, Physica C: Superconductivity and its Applications **445-448**, 94 (2006), ISSN 09214534, URL <https://www.sciencedirect.com/science/article/abs/pii/S092145340600236X>.
- [12] H. Eskes, G. Sawatzky, and L. Feiner, Physica C: Superconductivity **160**, 424 (1989), ISSN 09214534, URL <https://linkinghub.elsevier.com/retrieve/pii/0921453489904152>.
- [13] E. B. Stechel and D. R. Jennison, Physical Review B **38**, 4632 (1988), ISSN 0163-1829, URL <https://link.aps.org/doi/10.1103/PhysRevB.38.4632>.
- [14] P. Virtanen, R. Gommers, T. E. Oliphant, M. Haberland, T. Reddy, D. Cournapeau, E. Burovski, P. Peterson, W. Weckesser, J. Bright, et al., Nature Methods **17**, 261 (2020), ISSN 1548-7105, publisher: Nature Publishing Group, URL <https://www.nature.com/articles/s41592-019-0686-2>.